Arabian Journal of Chemistry (2022) **15**, 103883

King Saud University

Arabian Journal of Chemistry

www.ksu.edu.sa
www.sciencedirect.com

ORIGINAL ARTICLE

Biosorption of lead (II) from aqueous solution using Cellulose-based Bio-adsorbents prepared from unripe papaya (Carica papaya) peel waste: Removal Efficiency, Thermodynamics, kinetics and isotherm analysis

Wilavan Jaihan [a], Vanee Mohdee [a], Sompop Sanongraj [b], Ura Pancharoen [a,*], Kasidit Nootong [c,*]

[a] *Separation and Mass Transfer Research Laboratory, Department of Chemical Engineering, Faculty of Engineering, Chulalongkorn University, Bangkok 10330, Thailand*
[b] *Department of Chemical Engineering, Faculty of Engineering, Ubon Ratchathani University, Warin Chamrap, Ubon Ratchathani 34190, Thailand*
[c] *Bio-Circular-Green-economy Technology & Engineering Center (BCGeTEC), Department of Chemical Engineering, Faculty of Engineering, Chulalongkorn University, Bangkok 10330, Thailand*

Received 28 November 2021; accepted 30 March 2022
Available online 05 April 2022

KEYWORDS

Lead;
Papaya;
Adsorption;
Wastewater;
RSM

Abstract This work focuses on the removal of lead from contaminated aqueous solutions using unripe papaya peel based bio-adsorbents (PP). Response surface methodology (RSM) based on Box-Behnken design (BBD) is employed to determine the independent variables. Optimum conditions proved to be 96.5 mg/L of initial lead concentration in solution, at pH 4 of aqueous solution, having adsorbent dosage of 14.6 g/L and contact time (3 h) which subsequently yielded the predicted and actual lead removal efficiencies of 100% and 97.54%, respectively. Adsorption isotherms and kinetics of lead adsorption using unripe papaya peel followed the Freundlich and pseudo-second-order models, indicating that the process of chemisorption occurred. The magnitude of the adsorption capacity of the pseudo-second-order model ($q_{e,cal}$ = 6.25 mg/g) was found to be comparable to the value obtained experimentally ($q_{e,cal}$ = 6.45 mg/g). Thermodynamic parameters were calculated in order to identify the phenomena of adsorption. The values of $\Delta H°$ and $\Delta S°$ are found to be 13.61 J/mol and 54.30 J/molȧK, respectively. The characteristics of unripe papaya peel

* Corresponding authors.
E-mail addresses: ura.p@chula.ac.th (U. Pancharoen), kasidit.n@chula.ac.th (K. Nootong).
Peer review under responsibility of King Saud University.

Production and hosting by Elsevier

https://doi.org/10.1016/j.arabjc.2022.103883

bio-adsorbents, analyzed via SEM/EDX, FTIR and BET, are also presented. Thus, the O-H and C-O functional groups contained in the unripe papaya peel waste were found to effectively adsorb lead from the aqueous medium. The average pore diameters, average pore volumes and average surface area of bio-adsorbents prepared from unripe papaya peel waste proved to be 9.046 nm, 0.0012 cm^3/g and 0.755 m^2/g, respectively.

1. Introduction

Lead (Pb), a soft blue-gray metallic element, has been widely used in diverse industrial areas such as paints, batteries, leaded glasses, fuels, pigments, photographic materials, petrochemicals and mining etc. (Suren et al., 2014). Lead is considered to be a cumulative poison and has been found to be hazardous at high levels. Due to its toxicity, lead can cause damage to the digestive tract, immune system, human circulatory system, liver and kidney (Ghaedi et al., 2018; Yu et al., 2020). In Thailand, lead contamination in aquatic systems has been observed in many places (Mingkhwan and Worakhunpiset, 2018; Kladsomboon et al., 2020; Kosanlavit, 2021). Thus, its contamination has been become a serious problem. Various methods, such as coagulation-flocculation, liquid–liquid extraction, ion exchange and electrochemical treatment, have been employed to separate lead from aqueous solutions (Naeem et al., 2009; Pang et al., 2011; Liu et al., 2013). However, the drawbacks of these techniques include high operating costs, time consuming, difficulty in scaling up and the generation of a large volume of toxic sludge (Abbaszadeh et al., 2016; Ariffin et al., 2017; Wu et al., 2011a,b).

Adsorption has been reported as a green and economical method for lead removal in aqueous systems (Li et al., 2019; Fu et al., 2021). It is considered to be a suitable process for the selective binding of metal at low concentration (Li et al., 2019). Recently, bio-based adsorbents from agricultural wastes e.g. potato peel, cucumber peel and banana peel have received heightened interest with respect to the removal of heavy metals from contaminated wastewater (Ali et al., 2016; Ramakul et al., 2012; Basu et al., 2017; Amin et al., 2018; Arampatzidou and Deliyanni, 2016). Such attention is owing to the presence of carboxyl and hydroxyl functional groups in lignocellulose, which play an important role in improving adsorption efficiency (Basu et al., 2017; Amin et al., 2018; Dawn and Vishwakarma, 2021; Arampatzidou and Deliyanni, 2016). Thus, bio-based adsorbents prepared from agricultural wastes are considered to be promising alternative materials and efficient adsorbents for target analysis on account of its high adsorption capacity, renewability, low-cost and eco-friendly properties. (Li et al., 2017; Wang et al., 2016).

Papaya (*Carica papaya*) is a tropical fruit cultivated widely in Southeast Asia, Central America, and tropical islands. Papaya is popular both as a food and juice. Papaya production in Thailand is about 1.3 to 2.0 ktons annually; approximately 90% of the total production is consumed domestically. Market surveys also indicate that roughly 85% to 90% of the domestic papaya is consumed as green (unripen) papaya for the popular dish called "somtum" (Srisompun et al., 2018). Such consumption leads to a massive amount of papaya peel waste to be managed. Many researchers have been investigated the removal of heavy metals via biosorption process using different parts of papaya waste e.g. seeds, leaves and peel as an adsorbent (Shooto and Naidoo, 2019; Raju et al., 2013; Abbaszadeh et al., 2015). It is noted that the use of papaya peel as bio-adsorbent for lead removal has been, to date, limited only to ripe papaya which results of these experiments have proved unsatisfactory. The percentages of lead removal using ripe papaya have been found to be in the range of 80–93%, such values are low in comparison to those obtained when using other parts of papaya (Abbaszadeh et al., 2015; Adie Gilbert et al., 2011; Raju et al., 2012). To the best of our knowledge, an investigation as regards the use of unripe papaya peel for lead removal in aqueous systems has not been carried out before.

Response surface methodology (RSM) is an effective statistical technique for evaluating optimum conditions of diverse processes, including adsorption (Singh and Bhateria, 2020; Davarnejad et al., 2018). Box-Behnken design (BBD) has also been found to be suitable for three or more variables. Herein, it has been applied to achieve the most accurate prediction results (Singh and Bhateria, 2020; Chowdhury et al., 2016; Uçurum et al., 2018). Singh and Bhateria (2020) applied BBD for evaluating the interactive effect of five variables on lead ion adsorption using Fe_3O_4NPs as adsorbents. Many works have successfully evaluated optimized conditions having four variables using BBD e.g. copper adsorption (Chowdhury et al., 2016) and zinc adsorption (Uçurum et al., 2018). RSM based on BBD has proved to be a feasible and competent method for optimization of adsorption parameters and minimizing the number of experiments.

This work intends to evaluate the performance of unripe papaya peel as the bio-based adsorbents (PP) to remove lead from aqueous solution. RSM based on BBD is therefore, applied to determine the optimal adsorption conditions. Moreover, independent variables are evaluated viz. (i) initial lead concentration, (ii) pH of feed solution, (iii) adsorbent dosage and (iv) contact time. Various techniques are carried out in order to examine the as prepared bio-adsorbents characteristics i.e. SEM/EDX, BET and FTIR. Isotherms, kinetics and thermodynamics of lead adsorption are analyzed to explain the mechanisms involved.

2. Materials and methods

2.1. Chemicals

Lead (II) nitrate solution ($Pb(NO_3)_2$) was used to prepare the aqueous lead solution. Nitric acid (HNO_3) and sodium hydroxide (NaOH) were used to adjust the acidity-basicity of solutions. All solutions were prepared using distilled water

(Lee Cier Huad Ltd., Part.). All chemicals are of analytical grade and used without further purification. Detailed descriptions of chemicals used are presented in Table 1.

2.2. Adsorbent preparation

First, green (unripe) papayas were obtained from the local market in Bangkok. Then, the papaya peel was removed from the fruit and washed with distilled water to remove dirt. Next, the peel was chopped into small pieces and dried at 343 K in an oven until the weight was constant. The dried papaya peel was subsequently crushed into powder using a mortar and pestle and then sieved with a 40-mesh screen to obtain the papaya peel based bio-adsorbents (PP). In Fig. 1, a schematic diagram of unripe papaya peel based bio-adsorbents preparation is depicted.

2.3. Adsorbent characterization

2.3.1. SEM/EDx

Scanning electron microscope (SEM-JEOL, JSM-IT300) coupled with energy-dispersive x-ray spectrum (EDX-Oxford, X-MaxN20) were carried out to study the morphology and analyze the elemental composition of the PP, before and after adsorption of lead. Before scanning, all samples were dried and coated with gold to enhance electron conductivity. The micrographs were examined at 150X magnification.

2.3.2. BETa

The Brunauer-Emmett-Teller (BET- Micromeritics, 3Flex) method was used to determine the specific surface area and pore volume of PP. The relative pressure (p/p_0) was 0.004–0.99 bar and 0.99–0.10 bar for adsorption and desorption, respectively. Temperature of the bath was kept at 77.376 K, in liquid N_2. Degassing temperature was carried out at 60 ^{o}C for 1,440 min.

2.3.3. FTIRa

Fourier transform infrared spectroscopy (FTIR- Bruker, INVENIO-S) was employed to characterize the functional groups of PP, before and after lead adsorption. Samples were analyzed via the ATR diamond method. The measurement wavelength was in the range of 400–4000 cm^{-1}.

Table 1 Detailed information of the materials used*.

Chemical name	Molecular formular	Molecular weight (g/mol)	Purity (wt%)	Source
Lead (II) nitrate solution	$Pb(NO_3)_2$	331.20	1000.0[a]	PanReac Applichem
Nitric acid	HNO_3	63.013	65.0	Merck
Sodium hydroxide	NaOH	39.997	98.0	Ajax Finechem

Note: [a] is the concentration of lead ion in a unit of mg/L.
*The physical properties data are from chemical bottle labels.

2.4. Lead adsorption using PP

The lead adsorption experiment was conducted using unripe papaya peel as adsorbent. Synthetic wastewater was prepared by dissolving analytical-graded of $Pb(NO_3)_2$ in distilled water; the solution contained lead from 10 to 100 mg/L. The conditions of pH (4 to 6), adsorbent dosage (0.1 to 1.0 g per 50 mL of solution) and contact time (1 to 3 h) were used during the experiment. Firstly, lead solution (50 mL) and adsorbents were mixed in 100 mL flasks using a magnetic stirrer bar at 200 rpm, for the given contact time, at room temperature (303 K). Then, the solution was filtered using Whatman filtered paper with an average pore size of 2.5 μm. The amount of lead in the solution was measured via atomic absorption spectrometry (AAS-AGILENT 280FS AA). In Fig. 2, a schematic diagram of lead adsorption procedures is depicted. Both adsorption capacity (q_e, mg/g) and lead removal efficiency (E, %) were calculated, according to Eqs. (1) and (2), respectively (Abbaszadeh et al., 2016):

$$q_e = \frac{C_0 - C_e}{m} \times V \tag{1}$$

$$E = \frac{C_0 - C_e}{C_0} \times 100 \tag{2}$$

where C_o and C_e are initial and final (equilibrium) concentration of lead (mg/L) in solution, V is the volume of solution (L), m is the dosage of adsorbent (g) and q_e is the adsorption capacity (mg/g).

2.5. Optimization of process parameters

RSM based BBD by Minitab 17 software was applied to optimize the process of lead adsorption using unripe papaya peel as bio-adsorbents. Four independent variables were investigated, including the initial lead concentration in the solution (X_1), pH of feed solution (X_2), adsorbent dosage (X_3) and contact time (X_4). As illustrated in Table 2, three levels were examined (-1, 0 + 1). In Table 3, the experimental conditions, including 3 repetitions at the center points, are demonstrated. The lead removal efficiency as the response variable (Y) was fitted via a second-order polynomial model, as in Eq.(3):

$$Y = \beta_0 + \sum_{j=1}^{k} \beta_j X_j + \sum\nolimits_{j=1}^{k} \beta_{jj} X_j^2 + \sum \sum_{i<j} \beta_{ij} X_i X_j + \varepsilon \tag{3}$$

where Y is the predicted response while β_0, β_1, β_2, β_k, and ε demonstrate the offset term, the linear effect, the squared effect, the interaction effect and the residual term, respectively. X_i and X_j represent the coded independent variables.

2.6. Isotherm study

The isotherm study was conducted by varying the initial concentration of lead in synthetic wastewater from 10 to 110 mg/L, under optimized conditions obtained from RSM. The experiment was performed by adding PP into 100 mL flasks containing lead solution (50 mL). Then, the contents were mechanically stirred at 200 rpm for a given time at room temperature (303 K). Next, the solutions were filtered using Whatman filtered paper having an average pore size of

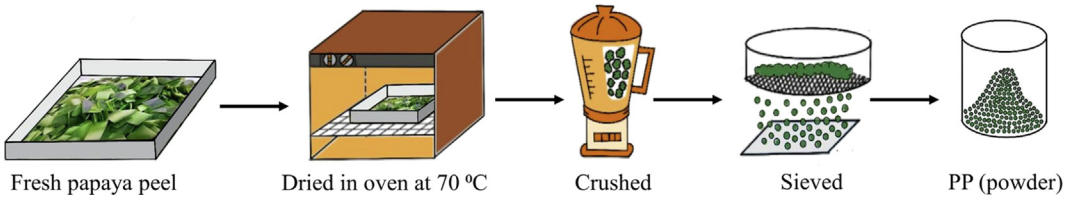

Fig. 1 Schema of papaya based bio-adsorbent (PP) preparation.

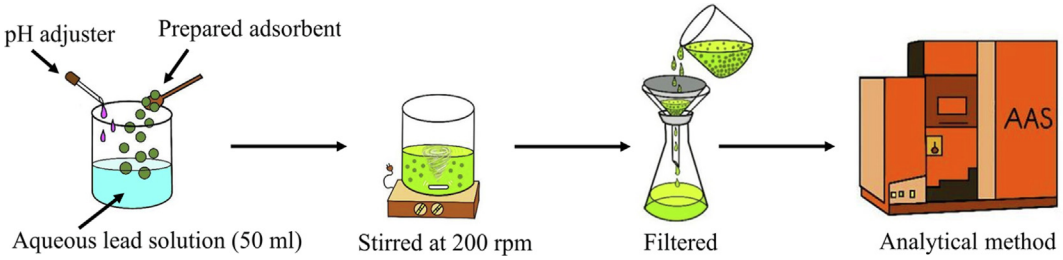

Fig. 2 Schema of lead adsorption procedure for PP.

Table 2 Investigated variables and their levels.

Parameter	Code	Level		
		−1	0	1
Initial lead concentration (mg/L)	X_1	10	55	100
pH of feed solution	X_2	4	5	6
Adsorbent dosage (g/50 mL)	X_3	0.1	0.55	1
Contact time (h)	X_4	1	2	3

Table 3 Experimental conditions for biosorption of lead unripe papaya peel based bio-adsorbents (PP).

Run	Experimental Condition				Run	Experimental Condition			
	X_1	X_2	X_3	X_4		X_1	X_2	X_3	X_4
1	10	4	0.55	2	15	55	4	1	2
2	100	4	0.55	2	16	55	6	1	2
3	10	6	0.55	2	17	10	5	0.1	2
4	100	6	0.55	2	18	100	5	0.1	2
5	55	5	0.1	1	19	10	5	1	2
6	55	5	1	1	20	100	5	1	2
7	55	5	0.1	3	21	55	4	0.55	1
8	55	5	1	3	22	55	6	0.55	1
9	10	5	0.55	1	23	55	4	0.55	3
10	100	5	0.55	1	24	55	6	0.55	3
11	10	5	0.55	3	25	55	5	0.55	2
12	100	5	0.55	3	26	55	5	0.55	2
13	55	4	0.1	2	27	55	5	0.55	2
14	55	6	0.1	2					

2.5 µm. The amount of lead in solution, before and after adsorption, was measured using AAS.

The data obtained from the experiment were linearly fitted for the Langmuir, Freundlich, Temkin, and Dubinin-Radushkevich (D-R) isotherms as described as follows:

2.6.1. Langmuir isotherm

The Langmuir isotherm quantitatively describes the monolayer adsorption on the outer surface of the adsorbent. No further adsorption takes place after the site was occupied; the adsorbate cannot permeate through the surface. The Langmuir isotherm can be expressed as follows (Dada et al., 2012):

$$\frac{1}{q_e} = \frac{1}{q_m} + \frac{1}{K_L q_m C_e} \tag{4}$$

where C_e is the equilibrium concentration of adsorbate (mg/L), q_e is the equilibrium adsorption capacity (mg/g), q_m is the maximum adsorption capacity (mg/g) and K_L is the Langmuir equilibrium constant (L/mg). The straight line was obtained by plotting $1/q_e$ versus $1/C_e$.

2.6.2. Freundlich isotherm

The Freundlich isotherm is an empirical adsorption model, which can be applied to nonideal biosorption on heterogeneous surfaces as well as multilayer sorption. The isotherm is displayed as shown in Eq.(5) (Varank et al., 2012; Nandiyanto et al., 2020):

$$\log q_e = \frac{1}{n} \log C_e + \log K_F \tag{5}$$

where K_F is the Freundlich constant related to the adsorption capacity and n is the constant describing the adsorption process. The value of $n = 1$ indicates a linear adsorption; $n < 1$ represents chemisorption, and $n > 1$ indicates the physical adsorption process (Nandiyanto et al., 2020; Desta, 2013). Both constants (K_F and n) can be calculated from the y-intercept and slope of the straight line of log q_e versus log C_e, respectively.

2.6.3. Temkin isotherm

The Temkin isotherm contains a factor that explicitly takes into account adsorbent-adsorbate interactions. As implied in the equation, its derivation is characterized by uniform distribution of binding energies, and is expressed in Eq. (6) (Dada et al., 2012):

$$q_e = B \ln K_T + B \ln C_e \quad (6)$$

where K_T is the Temkin isotherm constant (mg/g) and B is the Temkin constant associated with the heat of adsorption (J/mol). The constants can be calculated by plotting the straight line between q_e and ln C_e to obtain the y-intercept and the slope, respectively.

2.6.4. Dubinin-Radushkevich (D-R) isotherm

The last isotherm is the D-R model, which describes the adsorption energy between adsorbate and adsorbent in terms of the adsorption potential (ε). The D-R isotherm model can be described by Eqs. (7) to (9) (Piccin et al., 2011):

$$\ln q_e = \ln q_s + K_D \varepsilon^2 \quad (7)$$

$$\varepsilon = RT \ln \left[1 + \frac{1}{C_e}\right] \quad (8)$$

$$E = \frac{1}{\sqrt{2K_D}} \quad (9)$$

where q_s is the maximum adsorption capacity (mg/g), K_D is the D-R isotherm constant (mol^2/kJ^2), ε is the Polanyi adsorption potential, T is temperature (K) and R is the universal gas constant (8.314 J/molṡK). E is the mean sorption free energy of adsorbate at the moment it is adsorbed on the solid surface from the bulk solution (kJ/mol). The value of K_D can be calculated from the slope by plotting the straight line between ln q_e and ε^2.

2.7. Kinetics study

In order to clarify the reaction order and rate controlling mechanism, the following linear kinetic models were employed.

2.7.1. Pseudo-first-order

The pseudo-first-order kinetic model assumes that the number of sites that solutes can occupy is proportional to the rate of adsorption. The model is written as in Eq.(10) (Abbaszadeh et al., 2016):

$$\ln (q_e - q_t) = \ln q_e - k_1 t \quad (10)$$

where q_t and q_e are adsorption capacities at time t and equilibrium (mg/g), t is contact time (min) and k_1 is pseudo-first-order rate constant (min^{-1}). The constants q_e and k_1 can be calculated from the y-interception and slope of the straight line between ln ($q_e - q_t$) versus t, respectively.

2.7.2. Pseudo-second-order

The pseudo-second-order kinetic model involves chemisorption, where the removal of adsorbate from bulk liquid is due to the physiochemical interaction between adsorbent and adsorbate (El-Naas and Alhaija, 2013). The adsorption rate is also related to the availability of active sites on the adsorbent (Ali et al., 2016). The pseudo-second-order kinetic model is shown as in Eq. (11) (Varank et al., 2012):

$$\frac{t}{q_t} = \frac{t}{q_e} + \frac{1}{k_2 q_e^2} \quad (11)$$

where k_2 is the pseudo-second-order rate constant (g/mgṡmin). The straight line was obtained by plotting t/q_t versus t.

2.7.3. Intraparticle diffusion

As for the intraparticle diffusion model, it is noted that intraparticle diffusion transport is the slowest step of adsorption process between adsorbate and adsorbent, as compared to film diffusion and pore diffusion (Ghasemi et al., 2014). The intraparticle diffusion model can be written as in Eq. (12) (Varank et al., 2012):

$$q_t = k_{id} t^{\frac{1}{2}} + C \quad (12)$$

where k_{id} is the rate constant of the intraparticle diffusion model (mg/gṡmin$^{1/2}$) and C is the y-intercept. The values of k_{id} and C were obtained from the slope and y-intercept of the straight line by plotting q_t versus $t^{1/2}$, respectively.

2.8. Thermodynamic study

The thermodynamic study of the lead adsorption process was carried out at 303, 323 and 343 K; the initial concentration of lead in the solution, pH of solution, dosage of adsorbent and contact time were maintained according to the optimal conditions via RSM. The change in the standard Gibbs free energy ($\Delta G°$) for the adsorption process can be calculated, as in Eq. (13) (Abbaszadeh et al., 2016):

$$\Delta G^{\circ} = -RT \ln k_c \quad (13)$$

where k_c is the distribution coefficient, T is the absolute temperature (K), and R is the gas constant. The change in the standard Gibbs free energy ($\Delta G°$) is related to the standard enthalpy and entropy changes ($\Delta H°$ and $\Delta S°$) via the Gibbs-Helmholtz equation ($\Delta G° = \Delta H° - T\Delta S°$). Thus, k_c becomes:

$$\ln k_c = \frac{\Delta S^{\circ}}{R} - \frac{\Delta H^{\circ}}{RT} \quad (14)$$

Eq. (14) is the Van't Hoff equation in linear form. Thus, plotting ln k_c versus $1/T$ yielded a straight line, whose slope and y-intercept yielded $\Delta S°$ and $\Delta H°$, respectively.

2.9. Desorption experiments

The process of desorption for the unripe papaya peel bioadsorbents was accomplished by varying the concentration of HNO_3 at 0.1, 0.5, 1, 3 and 5 M (Chatterjee and Abraham, 2019). After the adsorption process, the adsorbed sample was mixed with HNO_3 for 3 h and then washed with distilled water five times. Thereafter, the sample was dried at 343 K in an oven until the weight was constant. The amount of desorbed lead can be calculated as in Eq.(15) (Abbaszadeh et al., 2016):

$$\%Desorption = \frac{Amount\ desorbed\ ion}{Amount\ adsorbed\ ion} \times 100 \quad (15)$$

3. Results and discussion

3.1. Characterization of adsorbent

3.1.1. SEM/ EDx

Fig. 3 displays SEM images of unripe papaya peel bioadsorbents before (PP) and after lead adsorption (PP-Pb). Before adsorption, PP was a bulky structure with large thick-

ness and had a smooth surface. A significantly rougher surface with a porous structure was observed after the adsorption of lead (Saleh et al., 2017). The presence of lead on the surface of PP was observed after adsorption, as indicated by the red dots (Fig. 3(b)). The results of EDX analysis (Table 4), showing the presence of lead after adsorption, confirmed that lead can be adsorbed on the surface of PP.

The elemental composition obtained from EDX analysis showed that generally elements were notices including C, O, K, Cl, Na and Ca which are frequently found in plant cells (Zvinowanda et al., 2010; Oladipo et al., 2020). The disappearance of Cl after adsorption might due to the detection limit refer to biological samples is quite low (Scimeca et al., 2018). Thus, the presence of heavy elements in the biological samples results in higher detection limits owing to the higher background 'noise' (Scimeca et al., 2018). Moreover, the concentration of Na and Ca increased slightly might be attributed to the uncertainty of EDX characterization, small amount of impurities within the distilled water, small amount of impurities to adjust the acidity-basicity of solutions and any impurities on the surface of laboratory glassware (Darvanjooghi et al., 2018).

3.1.2. BET

In Fig. 4, the N_2 adsorption–desorption isotherms of PP are depicted. According to the IUPAC system, the results were found to be type IV isotherm that exhibited an H_3 hysteresis loop at $0.5 < p/p_0 < 1.0$. The N_2 adsorption on PP exhibited a slit like pore structure (Fu and Huang, 2018). Further, the Barrett-Joyner-Halenda (BJH) average pore diameters of PP proved to be 9.046 nm. The values of the average pore diameters determined that PP had a mesoporous structure with respect to IUPAC classification (Fatombi et al, 2019). In addition, the average pore volume of PP was 0.0012 cm^3/g. The BET analysis yielded an average surface area of 0.755 m^2/g for PP, which is significantly lower than the absorbents prepared from ripe papaya peel (9.63 m^2/g) or activated carbon based papaya peel (15.28 m^2/g) (Abbaszadeh et al., 2015; Abbaszadeh et al., 2016). It is significant that the lower surface area was linked to the surface morphology of PP (bulky smooth structure) observed before adsorption. This is in contrast to previous works, which reported that the surface morphology of ripe papaya peel and papaya peel activated carbon adsorbents were highly porous and had uneven surfaces (Abbaszadeh et al., 2015; Abbaszadeh et al., 2016). Thus, the differences in adsorbent preparation resulted in different characteristic of the prepared adsorbent. For instance, higher surface areas of 9.63 and 15.28 m^2/g were obtained from previous works due to the raw material (ripened papaya peel) has been pretreated before the drying step i.e. boiled and then heated at high temperature followed by the surface modification with chemical solution (Abbaszadeh et al., 2015; Abbaszadeh et al., 2016).

Hence, the adsorption behavior is affected by various factors such as functional groups contained in the material, characteristic of adsorbent and operating conditions in the process. Darvanjooghi et al., (2018) stated that the pH of aqueous solution is one of the most important variables affecting the adsorption process. Moreover, the unripe papaya peel contains an enzyme namely; papain which exhibits the potential to bind with metals ions in the solution (He et al., 2010; Cahyaningrum et al., 2013). Previous studied also reported high performance of adsorption percentages using quite low surface area of prepared adsorbents (Amarasinghe and Williams, 2007; Feng and Guo, 2012).

3.1.3. FTIR

The FTIR spectra of PP and PP-Pb are illustrated in Fig. 5. It is acknowledged that the hydroxyl (O-H) functional groups contained in the agricultural wastes were able to adsorb heavy metals from the aqueous medium (Basu et al., 2017; Dawn and Vishwakarma, 2021). It is noted that the peak of the hydroxyl groups (O-H) of primary alcohol shifted from 1,030 to 1,025 cm^{-1} (Iqbal et al., 2009; Oikonomopoulos et al., 2010). As for the C-O of polysaccharide, the band shifted from 1,197 to 1,145 cm^{-1} (Gómez-Ordóñez and Rupérez, 2011; Fanta and Salch, 1991). The shifts of these peaks signify that both O-H and C-O were the main functional groups contributing to the binding of lead on the surface of the prepared adsorbent during the process of biosorption (Abbaszadeh et al., 2015; Abbaszadeh et al., 2016; Iqbal et al., 2009). The changes in intensity of the peaks demonstrated the interaction between the adsorbent surface of the functional groups and the metal ions in the aqueous solution (Abbaszadeh et al., 2015; Iqbal et al., 2009). The broad band around 3,239 cm^{-1} is assigned to O-H stretching, indicating a high content of alcohol and phenolic-OH functional groups in PP (Chen et al, 2015). The bands at 2,850 and 2,918 cm^{-1} correspond to the C-H stretching, indicating the presence of polysaccharide compounds (Fatombi et al, 2019). The band observed around 1,729 cm^{-1} is attributed to the C = O stretching (Yargıç et al, 2015). Moreover, the band at 1,238 cm^{-1} is characteristic of the

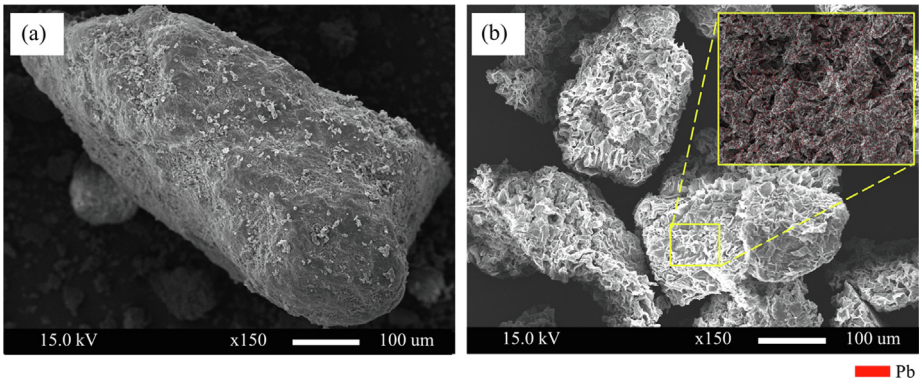

Fig. 3 SEM coupled with EDX of PP surface morphology: (a) before lead adsorption and (b) after lead adsorption.

Table 4 EDX analysis of unripe papaya based-bio adsorbents before and after lead adsorption.

Elements	Mass (%wt)	
	Before adsorption	After adsorption
C	51.50	43.67
O	43.69	49.49
K	3.54	1.04
Pb	–	1.56
Cl	1.27	–
Na	–	3.44
Ca	–	0.80

C = O stretching vibration in tertiary amides, suggesting that PP contains protein (Fatombi et al, 2019). The band around 1,197 cm^{-1} is associated with the C-O stretching vibration from polysaccharide (Gómez-Ordóñez and Rupérez, 2011; Fanta and Salch, 1991). The bands at 1,318 and 1,030 cm^{-1} are assigned to C-N stretching and the C-O stretching of alcohol and lignin (Li et al., 2019; Fatombi et al, 2019; Iqbal et al., 2009). The wave number which ranged from 950 to 1,200 cm^{-1} is considered to be the finger printed region of the carbohydrates (Chen et al, 2015).

3.2. Statistical analysis of biosorption of lead

3.2.1. RSM based on BBD approach

A regression equation as a function of the response (%E) and independent variables can be expressed as follows in Eq.(16):

$$\begin{aligned}\%E = {} & 81.4300 - 0.0334X_1 + 3.4700X_2 + 16.1900X_3 \\ & + 0.1800X_4 - 0.0004X_1X_1 - 0.2200X_2X_2 \\ & - 15.3100X_3X_3 - 0.1580X_4X_4 - 0.0221X_1X_2 \\ & + 0.2649X_1X_3 + 0.0159X_1X_4 - 0.9020X_2X_3 \\ & + 0.2730X_2X_4 - 1.3490X_3X_4\end{aligned} \quad (16)$$

In Table 5, the experimental and predicted values of removal percentages are reported. In Fig. 6, the predicted values of lead adsorption are plotted against the actual experimental data from run numbers 1 to 27, yielding the R^2 value of 0.9805, which verified the accuracy of the models and can be applied in the experiment. The high lead removal efficiencies from 83.56% to 99.87% were also obtained from the experimental run numbers: 1 to 27, which were subject to different operating conditions. Results obtained were slightly higher than the values from the ripe papaya peel adsorbents but were comparable to the results using papaya peel activated carbon or papaya peel adsorbent loaded with ferrous nanoparticles (Abbaszadeh et al., 2015; Abbaszadeh et al., 2016; Abbaszadeh et al., 2017).

In Table 6, ANOVA analyses are presented. The significance of the coefficient terms depends on the P-value and the F-value. A P-value < 0.05 is considered to be statistically significant (Singh and Bhateria, 2020; Alkarkhi, 2021). Further, previous studies have reported that when the P-value = 0.00, it is also significant (Ekpenyong et al, 2017). A high value of F indicates that most of the variables in the response can be explained by a regression equation. In Table 6, a high magnitude of F-value (42.99) is observed. Such a magnitude is seen to verify the fact that the independent variables in the model equation contributed to the removal of lead (Singh and Bhateria, 2020; Uçurum et al., 2018). Further, a lack-of-fit test is used to analyze whether the model fit is appropriate (Aliyu, 2019). The lack-of-fit of the model was found to be insignificant (P-value = 0.12, > 0.05), implying that 12% lack-of-fit was possibly due to the noise (Rai et al., 2019; Sharma et al., 2009). Herein, the following significant terms: X_1 (initial lead concentration), X_3 (adsorbent dosage), X_4 (contact time), X_1X_1 (self-interaction of initial lead concentration), X_3X_3 (self-interaction of adsorbent dosage), X_1X_2 (interaction between initial lead concentration and pH of feed solution) and X_1X_3 (interaction between initial lead concentration and adsorbent dosage) cannot be ignored.

3.2.2. Optimization of adsorption process

In Fig. 7, the optimization plots for lead adsorption using PP as an adsorbent are presented. By varying the concentration of lead in the range of 10 to 100 mg/L, the removal of lead decreased from 97.50 to 85.00%. Such a decrease in lead removal is attributed to the specific sites, which are saturated and to the exchange sites that are filled (Raju et al., 2012).

Consequently, the influence of pH of feed solution was also determined. Owing to the competition between lead ions and H^+ ions for appropriate sites on the adsorbent surfaces, maximum percentage for lead removal was seen to yield at pH 4, which was in agreement with previous studies (Raju et al., 2012; Darvanjooghi et al., 2018). Preliminary studies were performed in the pH range of 2–10; results are given in the supplementary material, **Fig. S1**. As shown, the maximum

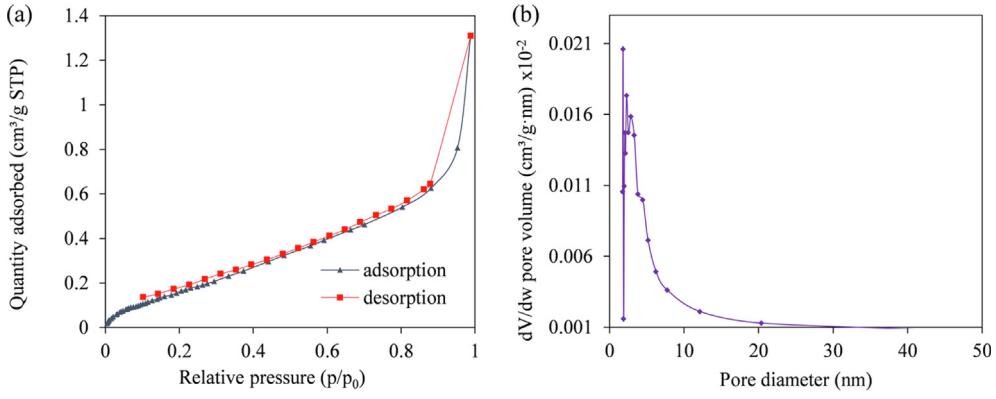

Fig. 4 BET analysis of N_2 adsorption–desorption isotherm (a) and pore-size distribution curves of PP (b).

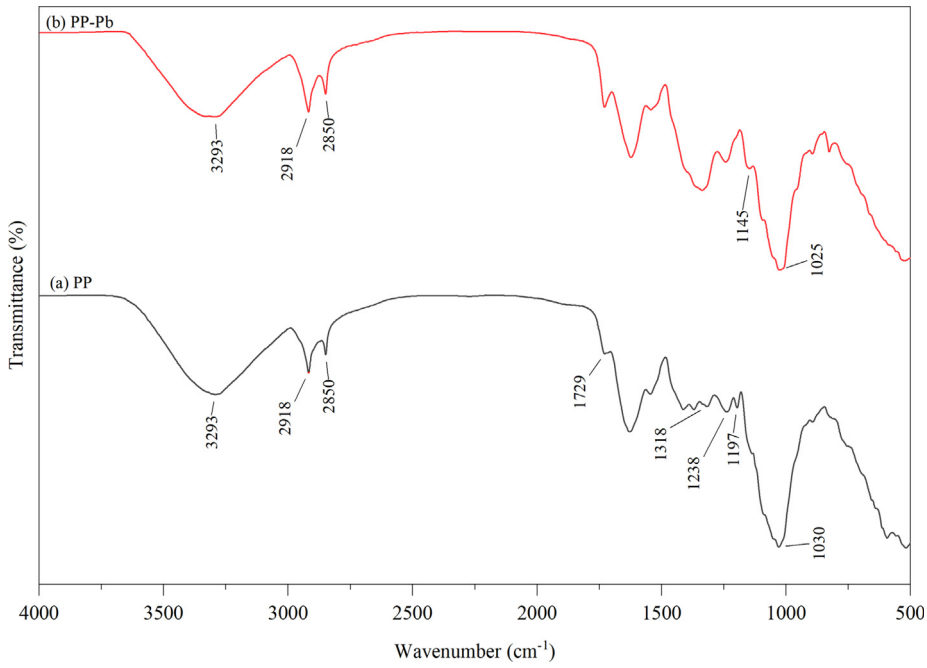

Fig. 5 Illustrate the results of FTIR before and after lead adsorption.

percentages of lead removal were observed at pH 4–6. In an acidic medium, the lower amount of lead adsorption on the adsorbents was due to the competition between lead and H^+ (Darvanjooghi et al., 2018). Thus, at the optimum pH of 4, lead ions were able to replace the H^+ bond, forming part of the surface functional groups such as –OH and –COOH (Raju et al., 2012). A downward trend in the removal percentages is noticed with further increased in pH value due to the formation of lead hydroxide resulting in the precipitation of lead in the solution (Abbaszadeh et al., 2015; Raju et al., 2012; Darvanjooghi et al., 2018; Kampalanonwat and Supaphol, 2014). Darvanjooghi et al., (2018) also reported that it is recommended to carry out experiments at pH 4 in order to avoid the precipitation of lead into the solution.

Table 5 Experimental and predicted values using RSM based on BBD for lead adsorption using unripe papaya based-bio adsorbents.

Run	% Removal		Run	% Removal	
	Experimental	Predicted		Experimental	Predicted
1	94.72	95.02	15	96.09	96.69
2	96.75	96.10	16	96.23	96.08
3	96.36	97.22	17	96.51	95.59
4	94.40	94.31	18	83.56	83.94
5	87.83	88.76	19	91.36	90.90
6	96.05	96.01	20	99.87	100.00
7	91.81	92.06	21	95.59	95.43
8	97.60	96.89	22	95.06	95.09
9	96.02	95.85	23	97.10	96.98
10	94.01	93.51	24	97.66	97.73
11	96.04	96.51	25	96.48	96.69
12	96.90	97.03	26	96.99	96.69
13	89.72	89.84	27	96.54	96.69
14	91.49	90.86			

Besides, when the dosage of adsorbent was increased from 0.1 to 1.0 g/50 mL, the removal of lead was found to increase from 85.00 to 97.50%. Hence, as the amount of dosage increased, the metal uptake of the adsorbent increased. It is evident that the removal of lead increased as the number of active sites increased, generated via the increase in dosage of the adsorbent (Raju et al., 2012).

Finally, the optimum time for lead adsorption was found to be 3 h. Removal percentages increased from 90% at 1 h of operation to 97.50% at 3 h of operation. At the initial stages, it is observed that removal percentages increased because more unsaturated surfaces and active sites were available on the surface areas of the adsorbents. As the process of adsorption proceeded, it is seen that more lead ions were adsorbed onto the surfaces (Abbaszadeh et al., 2016).

Applying Minitab software, the optimal conditions for the independent variables were identified: namely, initial lead concentration in wastewater at 96.5 mg/L, pH of wastewater at 4, adsorbent dosage at 0.73 g/50 mL (14.6 g/L) and contact time at 3 h. Thus, predicted and experimental values of lead removal efficiency were found to be 100% and 97.54%, respectively. Adsorption capacity under the optimized conditions proved to be 6.45 mg/g. It is noted that lead adsorption capacity remained significantly lower, as previously reported, when ripe papaya peel adsorbents were used (Abbaszadeh et al., 2015). This means that higher amounts of adsorbent dosage were required for PP. Nonetheless, the clear advantage associated with using unripe papaya peel adsorbents was the ease of adsorbent preparation without any surface modification and much lower costs involved.

3.2.3. Interpretation of three-dimensional surface plots

In Fig. 8, three-dimensional surface plots of lead removal efficiency as a function of independent variables are displayed. Interaction between the adsorbent dosage (X_3) and the remaining variables yielded apparent changes in lead removal

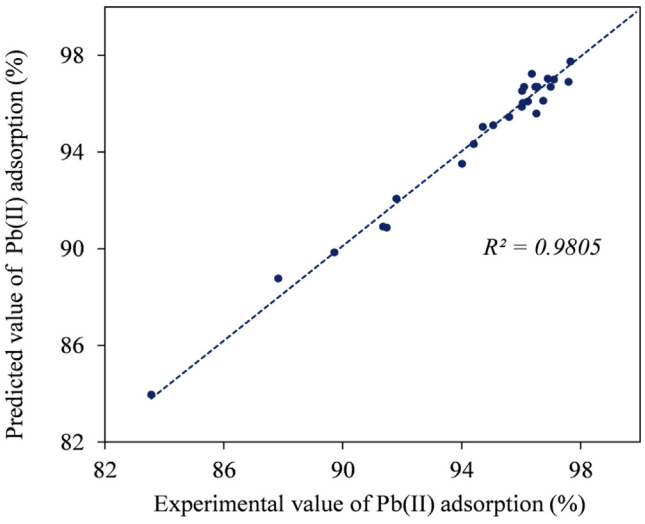

Fig. 6 Fitting qualities between experimental and predicted values.

efficiency. This is in contrast to the interaction between initial lead concentration (X_1) and pH of wastewater (X_2) and the interaction between initial lead concentration (X_1) and contact time (X_4), which resulted in relatively unchanged response curves. The results of the three-dimensional plots concurred with the ANOVA analysis, indicating the importance of adsorbent dosage on the percentage of lead removal.

3.3. Biosorption mechanism

The hydroxyl groups in cellulose are capable of being chemically modified by many reagents. In Fig. 9, the adsorption of lead on the surface of cellulose in the unripe papaya peel based bio-adsorbents occurred via –OH group (Adel, 2016). Thus, the formation of covalent bonds led to the adsorption of lead on the cellulose surface. Additionally, it has been reported that the unripe fruit of Carica papaya contains an important ingredient *viz*. papain, a thiol enzyme (He et al., 2010). Hence, papain is exhibited a potential for the selective binding of metal in an aqueous medium as well as the use in metal-chelated affinity separation. Previous research has shown that papain can react positively with various types of heavy metals (He et al., 2010; Cahyaningrum et al., 2013). Therefore, the unripe papaya peel is a good candidate than ripe papaya peel on account of its natural abundance waste, its ease of preparation and much lower costs involved.

Table 6 ANOVA analyses.

Source	Degree of freedom	Sum of squares	Mean square	F-value	P-value
Model	14	307.13	21.94	42.99	0.00
Linear	4	125.35	31.34	61.42	0.00
X_1	1	2.53	2.53	4.96	0.05
X_2	1	0.13	0.13	0.25	0.63
X_3	1	109.65	109.65	214.90	0.00
X_4	1	13.04	13.04	25.56	0.00
Square	4	58.20	14.55	28.51	0.00
X_1X_1	1	3.46	3.46	6.77	0.02
X_2X_2	1	0.26	0.26	0.50	0.49
X_3X_3	1	51.26	51.26	100.45	0.00
X_4X_4	1	0.13	0.13	0.26	0.62
2-Way interaction	6	123.57	20.60	40.36	0.00
X_1X_2	1	3.97	3.97	7.77	0.02
X_1X_3	1	115.12	115.12	225.61	0.00
X_1X_4	1	2.06	2.06	4.03	0.07
X_2X_3	1	0.66	0.66	1.29	0.28
X_2X_4	1	0.30	0.30	0.58	0.46
X_3X_4	1	1.48	1.48	2.89	0.12
Error	12	6.12	0.51	N/A	N/A
Lack-of-fit	10	5.97	0.60	7.70	0.12
Pure error	2	0.16	0.08	N/A	N/A
Total	26	313.25	N/A	N/A	N/A

3.4. Adsorption isotherm

The results of lead adsorption applying PP were correlated using the Langmuir, Freundlich, Temkin and D-R isotherms. The fit of the model with the experimental results was evaluated using linear regression analysis (as seen in the Supplementary material, **Fig. S2**). Thus, it is noted that the R^2 obtained from the Freundlich isotherm was the highest. Such a high value indicated that the Freundlich isotherm was the best

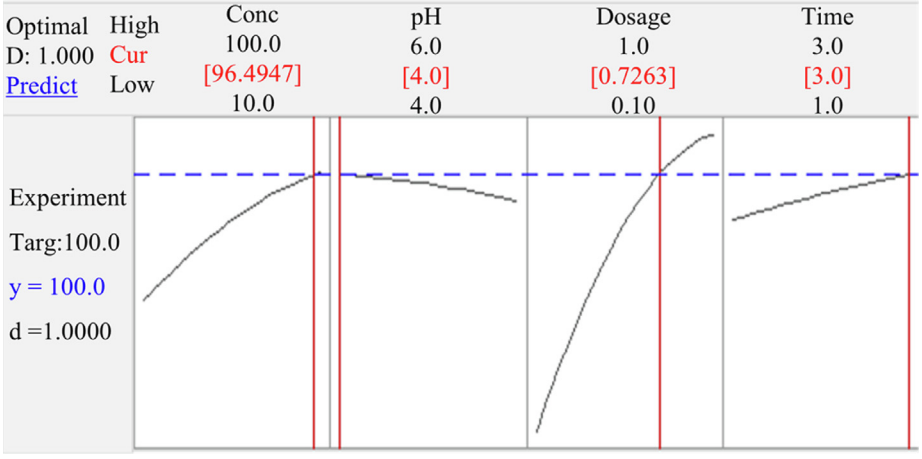

Fig. 7 Optimization plots for lead adsorption.

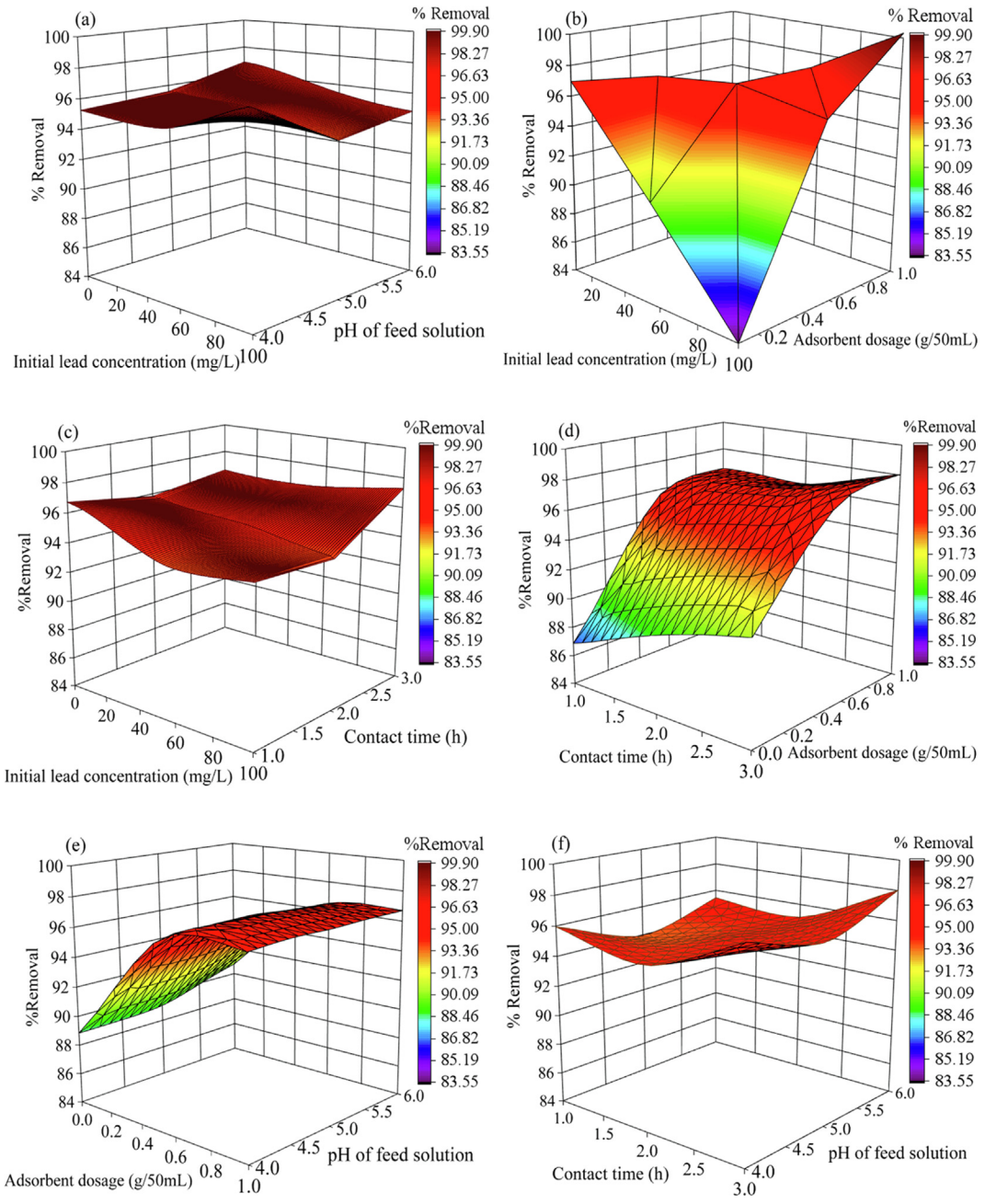

Fig. 8 Three-dimensional plots of (a) initial lead concentration and pH of feed solution (b) initial lead concentration and adsorbent dosage (c) initial lead concentration and contact time (d) contact time and adsorbent dosage (e) adsorbent dosage and pH of feed solution and (f) contact time and pH of feed solution.

model for lead adsorption, suggesting multilayer adsorption on the heterogeneous surface (Dada et al., 2012). Similar results were reported when adsorbents from ripe papaya peel were used to remove lead from an aqueous solution (Abbaszadeh et al., 2015). The value of n in this study was found to be 0.784, signifying that chemisorption took place (Nandiyanto et al., 2020; Desta, 2013). Yet, the values of the Langmuir parameters (q_m and K_L) were found to be negative; such negative results are perhaps due to the electrostatic nature of the process of adsorption (Huang et al., 2013; Ku and Caliskan, 2009; Özcan et al., 2004).

3.5. Adsorption kinetic

In the supplementary material, **Fig. S3**, the linear regression analysis and kinetic parameters of pseudo-first-order, pseudo-second-order and intraparticle diffusion models are given. Results revealed that the pseudo-second-order model yielded a higher correlation coefficient (R^2 = 0.998) than the pseudo-first-order and the intraparticle diffusion models. This observation indicated that the pseudo-second-order was the most suitable model for lead adsorption using unripe papaya peel. Results also suggest that chemical adsorption was the

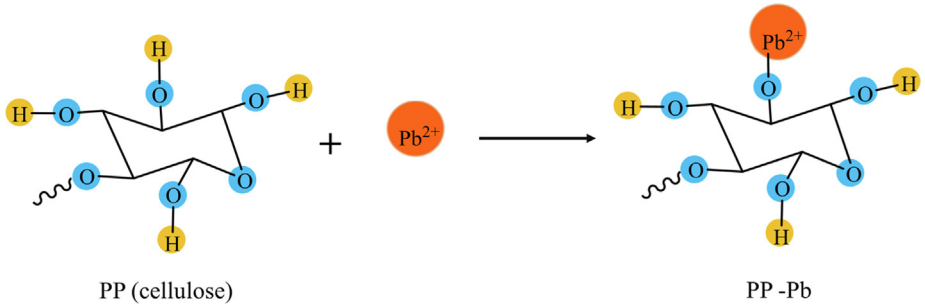

Fig. 9 Possible reaction mechanisms of PP with lead.

rate determining step of the process (Ali et al., 2016). This aligns with the work of previous researchers, who have reported pseudo-second-order to be the best fit model for metal adsorption when using adsorbents prepared from biomass containing tannin (Abbaszadeh et al., 2016; Ramakul et al., 2012; Şengil and Özacar, 2009). Moreover, the magnitude of the adsorption capacity of the pseudo-second-order model ($q_{e,cal}$ = 6.25 mg/g) was found to be comparable to the value obtained experimentally (q_e = 6.45 mg/g) under the optimized conditions via RSM. Such a result confirmed the validity of the pseudo-second-order, proving that the kinetic model applied for lead adsorption using PP was the most suitable. As for the intraparticle diffusion model, its low correlation coefficient (R^2 = 0.7701) suggests that the adsorption process was not controlled by intraparticle diffusion as normally reported for other porous materials (Carvalho et al., 2018; Cheng et al., 2013). Due to the relatively smooth surface morphology of the prepared bio-adsorbents, it is possible to conclude that the intraparticle diffusion of lead into the adsorbent was unlikely.

3.6. Thermodynamic study

In the supplementary material, **Fig. S4**, and Table 7, plots are displayed of ln k_c versus $1/T$ that consequently yielded the values of $\Delta H°$ and $\Delta S°$ at 13.61 J/mol and 54.30 J/molȧK, respectively. A positive value of $\Delta H°$ was observed indicating that the process of adsorption was endothermic. Previous research also reported the same outcome of an endothermic lead adsorption process when employing papaya seeds as bio-adsorbents (Yadav et al., 2014; Olu-Owolabi et al., 2018). Such a result can be explained given that the total energy released in bond breaking was lower than the total energy adsorbed in bond making between the lead and adsorbent (Mousavi et al., 2010; Abubakar et al., 2020). The positive value of $\Delta S°$ indicated an increase in randomness at the adsorbent-solution interface (Kumar et al., 2019). Negative values of $\Delta G°$, however, demonstrated that the adsorption process was both thermodynamic and spontaneous, which is quite feasible; the increase of $\Delta G°$ with temperature implies that the process favors higher energy input (Abbaszadeh et al., 2016).

Table 7 Thermodynamic parameters for lead adsorption.

Δ^0G (kJ/mol)			Δ^0H (J/mol)	Δ^0S (J/mol K)
303 K	323 K	343 K		
−2.941	−3.703	−5.142	13.612	54.304

3.7. Desorption study

Desorption experiments were evaluated by varying the concentration of HNO_3. It is noted that the amount of excessive protons in HNO_3 solution was seen to react with the adsorbent and can disrupt the bonds of adsorbate and adsorbent (Chatterjee and Abraham, 2019). Results found that the highest desorption efficiency was obtained at 3 M, as shown in **Fig. S5**. The desorption efficiency of PP was found to be 77.16%.

4. Conclusion

In this paper, results demonstrate that bio-adsorbents prepared from unripe papaya peel waste can effectively remove lead from aqueous solution. Herein, percentages of predicted and actual lead removal efficiencies reached 100% and 97.54%, respectively. Besides, isotherm and kinetic analyses revealed that Freundlich and pseudo-second-order models were best suited for the process of lead adsorption using unripe papaya peel based bio-adsorbents. Thermodynamic parameters proved that the process was both endothermic and spontaneous. Although the adsorption capacity was slightly lower than the values from the modified adsorbents prepared from ripen papaya peel, the ease of preparation and the likely lower expense associated with the process are clear advantages. Finally, this work underlines the case of utilizing agricultural waste and environmental friendly processes to remove pollutants from aqueous solutions.

CRediT authorship contribution statement

Wilavan Jaihan: Methodology, Data curation, Investigation, Writing - original draft. **Vanee Mohdee:** Validation, Writing - review & editing. **Sompop Sanongraj:** Project administration. **Ura Pancharoen:** Supervision, Conceptualization, Funding acquisition. **Kasidit Nootong:** Project administration, Validation, Writing - review & editing.

Declaration of Competing Interest

The authors declare that they have no known competing financial interests or personal relationships that could have appeared to influence the work reported in this paper.

Acknowledgement

The authors profoundly appreciate the financial support by the 90th Anniversary of Chulalongkorn University Fund (Ratchadaphiseksomphot Endowment Fund), the Department of Chemical Engineering Fund (Faculty of Engineering, Chulalongkorn University for Master's Degree students) and the Research Cess Fund (Malaysia-Thailand Joint Authority), the Thailand Science Research and Innovation Fund Chulalongkorn University (CU_FRB65_bcg(25)_139_21_05). Sincere thanks also are extended to the Separation Laboratory (Department of Chemical Engineering, Faculty of Engineering, Chulalongkorn University) for their help and support. And authors gratefully thanks also go to Dr. Thidarat Wongsawa for her kind help.

Appendix A. Supplementary material

Supplementary data to this article can be found online at https://doi.org/10.1016/j.arabjc.2022.103883.

References

Abbaszadeh, S., Alwi, S.R.W., Ghasemi, N., Nodeh, H.R., Webb, C., Muhamad, I.I., 2015. Use of pristine papaya peel to remove Pb(II) from aqueous solution. Chem. Eng. Trans. 45, 961–966. https://doi.org/10.3303/CET1545161.

Abbaszadeh, S., Rashidi Nodeh, H., Wan Alwi, S.R., 2017. Bio-adsorbent derived from papaya peel waste and magnetic nanoparticles fabricated for lead determination, Pure Appl. Chem. 90, 79–92. https://doi.org/10.1515/pac-2017-0503.

Abbaszadeh, S., Wan Alwi, S.R., Webb, C., Ghasemi, N., Muhamad, I.I., 2016. Treatment of lead-contaminated water using activated carbon adsorbent from locally available papaya peel biowaste. J. Clean. Prod. 118, 210–222. https://doi.org/10.1016/j.jclepro.2016.01.054.

Abubakar, A., Sabo, I.A., Yahuza, S., 2020. Thermodynamics Modelling of Lead (II) Biosorption using Cystoseira stricta Biomass. BSTR. 8, 21–23.

Adel, A., 2016. Incorporation of nano-metal particles with paper matrices. Interdiscip. J. Chem. 1, 36–46. https://doi.org/10.15761/IJC.1000107.

Adie Gilbert, U., Unuabonah Emmanuel, I., Adeyemo Adebanjo, A., Adeyemi Olalere, G., 2011. Biosorptive removal of Pb^{2+} and Cd^{2+} onto novel biosorbent: Defatted Carica papaya seeds. Biomass Bioenergy. 35, 2517–2525. https://doi.org/10.1016/j.biombioe.2011.02.024.

Ali, R.M., Hamad, H.A., Hussein, M.M., Malash, G.F., 2016. Potential of using green adsorbent of heavy metal removal from aqueous solutions: Adsorption kinetics, isotherm, thermodynamic, mechanism and economic analysis. Ecol. Eng. 91, 317–332. https://doi.org/10.1016/j.ecoleng.2016.03.015.

Aliyu, A., 2019. Synthesis, electron microscopy properties and adsorption studies of Zinc(II) ions (Zn^{2+}) onto as-prepared carbon nanotubes (CNTs) using Box-Behnken design (BBD). Sci. Afr. 3,. https://doi.org/10.1016/j.sciaf.2019.e00069 e00069.

Alkarkhi, A.F.M., 2021. 6 - The observed significance level (P-value) procedure. In: Alkarkhi, A.F.M. (Ed.), Applications of hypothesis testing for environmental science. Elsevier, pp. 79–119.

Amarasinghe, B.M.W.P.K., Williams, R.A., 2007. Tea waste as a low cost adsorbent for the removal of Cu and Pb from wastewater. Chem. Eng. J. 132, 299–309. https://doi.org/10.1016/j.cej.2007.01.016.

Amin, M.T., Alazba, A.A., Shafiq, M., 2018. Removal of copper and lead using banana biochar in batch adsorption systems: isotherms and kinetic studies. Arab. J. Sci. Eng. 43, 5711–5722. https://doi.org/10.1007/s13369-017-2934-z.

Ariffin, N., Abdullah, M.M.A.B., Rozainy, Z., Murshed, M.F., Zain, H., Meor Ahmad Tajudin, M.A.F., Bayuaji, R., 2017. Review on adsorption of heavy metal in wastewater by using geopolymer, MATEC Web Conf. 97, 01023. https://doi.org/10.1051/matecconf/20179701023.

Arampatzidou, A.C., Deliyanni, E.A., 2016. Comparison of activation media and pyrolysis temperature for activated carbons development by pyrolysis of potato peels for effective adsorption of endocrine disruptor bisphenol-A. J. Colloid. Interface. Sci. 466, 101–112. https://doi.org/10.1016/j.jcis.2015.12.003.

Basu, M., Guha, A.K., Ray, L., 2017. Adsorption of lead on cucumber peel. J. Clean. Prod. 151, 603–615. https://doi.org/10.1016/j.jclepro.2017.03.028.

Cahyaningrum, S.E., Narsito, S., Santosa, R.A., 2013. Preparation and properties of papain immobilized onto metal ions cross-linked chitosan beads. Res. J. Pharm. Biol. Chem. Sci. 4, 120–126.

Carvalho, L., Chagas, P., Pinto, L., 2018. Caesalpinia ferrea fruits as a biosorbent for the removal of Methylene Blue dye from an aqueous medium. Water Air Soil Pollut. 229, 297. https://doi.org/10.1007/s11270-018-3952-5.

Chatterjee, A., Abraham, J., 2019. Desorption of heavy metals from metal loaded sorbents and e-wastes: A review. Biotechnol. Lett. 41, 319–333. https://doi.org/10.1007/s10529-019-02650-0.

Chen, H.M., Fu, X., Luo, Z.G., 2015. Esterification of sugar beet pectin using octenyl succinic anhydride and its effect as an emulsion stabilizer. Food Hydrocoll. 49, 53–60. https://doi.org/10.1016/j.foodhyd.2015.03.008.

Cheng, C.S., Deng, J., Lei, B., He, A., Zhang, X., Ma, L., Li, S., Zhao, C., 2013. Toward 3D graphene oxide gels based adsorbents for high-efficient water treatment via the promotion of biopolymers. J. Hazard. Mater. 263, 467–478. https://doi.org/10.1016/j.jhazmat.2013.09.065.

Chowdhury, Z.Z., Abd Hamid, S.B., Rahman, M.M., Rafique, R.F., 2016. Catalytic activation and application of micro-spherical carbon derived from hydrothermal carbonization of lignocellulosic biomass: Statistical analysis using Box-Behnken design. RSC Adv. 6, 102680–102694. https://doi.org/10.1039/C5RA26189A.

Dada, A.O., Olalekan, A.P., Olatunya, A.M., Dada, O., 2012. Langmuir, Freundlich, Temkin and Dubinin-Radushkevich Isotherms studies of equilibrium sorption of Zn^{2+} unto phosphoric acid modified rice husk. J. Appl. Chem. 3, 38–45. https://doi.org/10.9790/5736-0313845.

Darvanjooghi, M.H.K., Davoodi, S.M., Dursun, A.Y., Ehsani, M.R., Karimpour, I., Ameri, E., 2018. Application of treated eggplant peel as a low-cost adsorbent for water treatment toward elimination of Pb^{2+}: Kinetic modeling and isotherm study. Adsorp. Sci. Technol. 36, 1112–1143. https://doi.org/10.1177/0263617417753784.

Davarnejad, R., Moraveji, M.K., Havaie, M., 2018. Integral technique for evaluation and optimization of Ni (II) ions adsorption onto regenerated cellulose using response surface methodology, Arabian. J. Chem. 11, 370–379. https://doi.org/10.1016/j.arabjc.2015.05.022.

Dawn, S.S., Vishwakarma, V., 2021. Recovery and recycle of wastewater contaminated with heavy metals using adsorbents incorporated from waste resources and nanomaterials-A review. Chemosphere. 273,. https://doi.org/10.1016/j.chemosphere.2021.129677 129677.

Desta, M.B., 2013. Batch sorption experiments: Langmuir and Freundlich Isotherm studies for the adsorption of textile metal ions onto Teff Straw (Eragrostis tef) agricultural waste. J. Thermodyn. 2013,. https://doi.org/10.1155/2013/375830 375830.

Ekpenyong, M., Antai, S., Asitok, A., Ekpo, B., 2017. Response surface modeling and optimization of major medium variables for glycolipopeptide production. Biocatal. Agric. Biotechnol. 10, 113–121. https://doi.org/10.1016/j.bcab.2017.02.015.

El-Naas, M., Alhaija, M.A., 2013. Chapter-12 Modelling of adsorption processes. In: Brennan, C.R. (Ed.), Mathematical modelling. Nova Publishers Inc., UAE, pp. 579–600.

Fanta, G.F., Salch, J.H., 1991. Analysis of polysaccharide-poly (ethylene-co-acrylic acid) composites by fourier-transform infrared spectroscopy. Carbohydr. Polym. 14, 393–409. https://doi.org/10.1016/0144-8617(91)90005-W.

Fatombi, J.K., Osseni, S.A., Idohou, E.A., Agani, I., Neumeyer, D., Verelst, M., Mauricot, R., Aminou, T., 2019. Characterization and application of alkali-soluble polysaccharide of Carica papaya seeds for removal of indigo carmine and Congo red dyes from single and binary solutions. J. Environ. Chem. Eng. 7,. https://doi.org/10.1016/j.jece.2019.103343 103343.

Feng, N.-C., Guo, X.-Y., 2012. Characterization of adsorptive capacity and mechanisms on adsorption of copper, lead and zinc by modified orange peel. Trans. Nonferrous Met. Soc. China. 22, 1224–1231. https://doi.org/10.1016/S1003-6326(11)61309-5.

Fu, C., Zhu, X., Dong, X., Zhao, P., Wang, Z., 2021. Study of adsorption property and mechanism of lead(II) and cadmium(II) onto sulfhydryl modified attapulgite. Arabian J. Chem. 14,. https://doi.org/10.1016/j.arabjc.2020.102960 102960.

Fu, W., Huang, Z., 2018. Magnetic dithiocarbamate functionalized reduced graphene oxide for the removal of Cu(II), Cd(II), Pb(II), and Hg(II) ions from aqueous solution: Synthesis, adsorption, and regeneration. Chemosphere. 209, 449–456. https://doi.org/10.1016/j.chemosphere.2018.06.087.

Ghaedi, A.M., Panahimehr, M., Nejad, A.R.S., Hosseini, S.J., Vafaei, A., Baneshi, M.M., 2018. Factorial experimental design for the optimization of highly selective adsorption removal of lead and copper ions using metal organic framework MOF-2(Cd). J. Mol. Liq. 272, 15–26. https://doi.org/10.1016/j.molliq.2018.09.051.

Ghasemi, M., Ghasemi, N., Zahedi, G., Wan Alwi, S.R., Goodarzi, M., Javadian, H., 2014. Kinetic and equilibrium study of Ni(II) sorption from aqueous solutions onto Peganum harmala-L. Int. J. Environ. Sci. Technol. 11, 1835–1844. https://doi.org/10.1007/s13762-014-0617-9.

Gómez-Ordóñez, E., Rupérez, P., 2011. FTIR-ATR spectroscopy as a tool for polysaccharide identification in edible brown and red seaweeds. Food Hydrocoll. 25, 1514–1520. https://doi.org/10.1016/j.foodhyd.2011.02.009.

He, Z.Y., Christopher, B.W., Zhou, Y.T., Nie, H.L., Zhu, L.M., 2010. Papain adsorption on chitosan-coated nylon-based immobilized metal ion (Cu^{2+}, Ni^{2+}, Zn^{2+}, Co^{2+}) affinity membranes. Sep. Sci. Technol. 45, 525–534. https://doi.org/10.1080/01496390903484784.

Huang, H., Fan, Y., Wang, J., Gao, H., Tao, S., 2013. Adsorption kinetics and thermodynamics of water-insoluble crosslinked β-cyclodextrin polymer for phenol in aqueous solution. Macromol. Res. 21, 726–731. https://doi.org/10.1007/s13233-013-1086-6.

Iqbal, M., Saeed, A., Zafar, S.I., 2009. FTIR spectrophotometry, kinetics and adsorption isotherms modeling, ion exchange, and EDX analysis for understanding the mechanism of Cd^{2+} and Pb^{2+} removal by mango peel waste, J. Hazard. Mater. 164, 161-171. https://doi.org/10.1016/j.jhazmat.2008.07.141.

Kampalanonwat, P., Supaphol, P., 2014. The study of competitive adsorption of heavy metal ions from aqueous solution by aminated polyacrylonitrile nanofiber mats, Energy Procedia. 56, 142–151. https://doi: 10.1016/j.egypro.2014.07.142.

Kladsomboon, S., Jaiyen, C., Choprathumma, C., Tusai, T., Apilux, A., 2020. Heavy metals contamination in soil, surface water, crops, and resident blood in Uthai District, Phra Nakhon Si Ayutthaya, Thailand. Environ. Geochem. Health. 42, 545–561. https://doi.org/10.1007/s10653-019-00388-2.

Kosanlavit, W., 2021. Efficiency and kinetic rate of nanoscale and microscale of zero valent iron and zinc oxide particles for chromium, cadmium, and lead removal from Pak Thong Chai silk dyeing effluent, Thailand. TURCOMAT. 12, 2690–2702. https://doi.org/10.17762/turcomat.v12i8.3941.

Kul, A.R., Caliskan, N., 2009. Equilibrium and kinetic studies of the adsorption of Zn(II) ions onto natural and activated kaolinites. Adsorpt. Sci. Technol. 27, 85–105. https://doi.org/10.1260/026361709788921632.

Kumar, R., Ansari, M.O., Alshahrie, A., Darwesh, R., Parveen, N., Yadav, S.K., Barakat, M.A., Cho, M.H., 2019. Adsorption modeling and mechanistic insight of hazardous chromium on para toluene sulfonic acid immobilized-polyaniline@CNTs nanocomposites. J. Saudi Chem. Soc. 23, 188–197. https://doi.org/10.1016/j.jscs.2018.06.005.

Li, M., Jiao, C., Yang, X., Wang, C., Wu, Q., Wang, Z., 2017. Solid phase extraction of carbamate pesticides with banana peel derived hierarchical porous carbon prior to high performance liquid chromatography. Anal. Methods. 9, 593–599. https://doi.org/10.1039/c6ay02678h.

Li, X., Wang, Z., Liang, H., Ning, J., Li, G., Zhou, Z., 2019. Chitosan modification persimmon tannin bioadsorbent for highly efficient removal of Pb(II) from aqueous environment: The adsorption equilibrium, kinetics and thermodynamics. Environ. Technol. 40, 112–124. https://doi.org/10.1080/09593330.2017.1380712.

Liu, Y., Yan, J., Yuan, D., Li, Q., Wu, X., 2013. The study of lead removal from aqueous solution using an electrochemical method with a stainless steel net electrode coated with single wall carbon nanotubes. Chem. Eng. J. 218, 81–88. https://doi.org/10.1016/j.cej.2012.12.020.

Mingkhwan, R., Worakhunpiset, S., 2018. Heavy metal contamination near industrial estate areas in Phra Nakhon Si Ayutthaya Province, Thailand and human health risk assessment. Int. J. Environ. Res. Public Health. 15, 1890. https://doi.org/10.3390/ijerph15091890.

Mousavi, H., Hosseynifar, A., Jahed, V., Dehghani, S., 2010. Removal of lead from aqueous solution using waste tire rubber ash as an adsorbent. Braz. J. Chem. Eng. 27, 79–87. https://doi.org/10.1590/S0104-66322010000100007.

Naeem, A., Saddique, M.T., Mustafa, S., Kim, Y., Dilara, B., 2009. Cation exchange removal of Pb from aqueous solution by sorption onto NiO. J. Hazard. Mater. 168, 364–368. https://doi.org/10.1016/j.jhazmat.2009.02.040.

Nandiyanto, A., Girsang, G., Maryanti, R., Ragadhita, R., Anggraeni, S., Fauzi, F., Sakinah, P., Astuti, A., Usdiyana, D., Dewi, M., Al-Obaidi, A.S., 2020. Isotherm adsorption characteristics of carbon microparticles prepared from pineapple peel waste. Commun. sci. technol. 5, 31–39. https://doi.org/10.21924/cst.5.1.2020.176.

Oikonomopoulos, I., Perraki, T., Tougiannidis, N., 2010. FTIR study of two different lignite lithotypes from Neocene Achlada lignite deposits in NW Greece. BGSG. 5, 2284–2293. https://doi.org/10.12681/bgsg.14312.

Oladipo, B., Ojumu, T.V., Latinwo, L.M., Betiku, E., 2020. Pawpaw (Carica papaya) peel waste as a novel green heterogeneous catalyst for Moringa oil methyl esters synthesis: Process optimization and kinetic study. Energies. 13, 5834. https://doi.org/10.3390/en13215834.

Olu-Owolabi, B.I., Diagboya, P.N., Unuabonah, E.I., Alabi, A.H., Düring, R.A., Adebowale, K.O., 2018. Fractal-like concepts for evaluation of toxic metals adsorption efficiency of feldspar-biomass composites. J. Clean. Prod. 171, 884–891. https://doi.org/10.1016/j.jclepro.2017.10.079.

Özcan, A.S., Erdem, B., Özcan, A., 2004. Adsorption of Acid Blue 193 from aqueous solutions onto Na-bentonite and DTMA-bentonite. J. Colloid Interface Sci. 280, 44–54. https://doi.org/10.1016/j.jcis.2004.07.035.

Pang, F.M., Kumar, P., Teng, T.T., Mohd Omar, A.K., Wasewar, K. L., 2011. Removal of lead, zinc and iron by coagulation-flocculation. J. Taiwan. Inst. Chem. Eng. 42, 809–815. https://doi.org/10.1016/j.jtice.2011.01.009.

Piccin, J., Dotto, G., Pinto, L., 2011. Adsorption isotherms and thermochemical data of FD and C Red N° 40 binding by chitosan, Brazilian. J. Chem. Eng. 28, 295–304. https://doi.org/10.1590/S0104-66322011000200014.

Rai, P., Pandey, A., Pandey, A., 2019. Optimization of sugar release from banana peel powder waste (BPPW) using box-behnken design (BBD): BPPW to biohydrogen conversion. Int. J. Hydrog. Energy. 44, 25505–25513. https://doi.org/10.1016/j.ijhydene.2019.07.168.

Raju, D., Kiran, G.R., Rao, D.V., 2013. Comparison studies on biosorption of lead (II) from an aqueous solution using anacardium occidentale and Carica papaya leaves powder. IJETED. 3, 273–283.

Raju, D.S.S.R., Rao, V.N., Prasad, P.R., Babu, N.C., 2012. Sorption of lead(II) ions from wastewater using carica papaya leaf powder. Int. J. Eng. Sci. Adv. Technol. 2, 1577–1581.

Ramakul, P., Yanachawakul, Y., Leepipatpiboon, N., Sunsandee, N., 2012. Biosorption of palladium(II) and platinum(IV) from aqueous solution using tannin from Indian almond (Terminalia catappa L.) leaf biomass: Kinetic and equilibrium studies. Chem. Eng. J. 193–194, 102–111. https://doi.org/10.1016/j.cej.2012.04.035.

Saleh, M., Assaad, F., Abdel-Salam, A.S., Youssef, R., El-Damarawy, Y., 2017. Adsorption of lead onto a waste biomaterial-biochar. Nat. sci. 15, 154–164. https://doi.org/10.7537/marsnsj151217.16.

Scimeca, M., Bischetti, S., Lamsira, H.K., Bonfiglio, R., Bonanno, E., 2018. Energy Dispersive X-ray (EDX) microanalysis: A powerful tool in biomedical research and diagnosis. Eur. J. Histochem. 62, 2841. https://doi.org/10.4081/ejh.2018.2841.

Şengil, İ.A., Özacar, M., 2009. Competitive biosorption of Pb^{2+}, Cu^{2+} and Zn^{2+} ions from aqueous solutions onto valonia tannin resin. J. Hazard. Mater. 166, 1488–1494. https://doi.org/10.1016/j.jhazmat.2008.12.071.

Sharma, S., Malik, A., Satya, S., 2009. Application of response surface methodology (RSM) for optimization of nutrient supplementation for Cr(VI) removal by Aspergillus lentulus AML05. J. Hazard. Mater. 164, 1198–1204. https://doi.org/10.1016/j.jhazmat.2008.09.030.

Shooto, N., Naidoo, E., 2019. Detoxification of wastewater by Paw-Paw (Carica papaya L.) seeds adsorbents. Asian J. Chem. 31, 2249–2256. https://doi.org/10.14233/ajchem.2019.22051.

Singh, R., Bhateria, R., 2020. Optimization and experimental design of the Pb^{2+} adsorption process on a nano-Fe_3O_4-based adsorbent using the response surface methodology. ACS Omega. 5, 28305–28318. https://doi.org/10.1021/acsomega.0c04284.

Srisompun, O., Sinsir, N., Simla, S., Boontang, S., Butso, W., 2018. Demands and consumption behavior of papaya salad restaurants in the mid northeastern part, Khon Kaen Agr. J. 46, 702–707.

Suren, S., Pancharoen, U., Kheawhom, S., 2014. Simultaneous extraction and stripping of lead ions via a hollow fiber supported liquid membrane: Experiment and modeling. J. Ind. Eng. Chem. 20, 2584–2593. https://doi.org/10.1016/j.jiec.2013.10.045.

Uçurum, M., Özdemir, A., Teke, C., Serencam, H., İpek, M., 2018. Optimization of adsorption parameters for Ultra-Fine calcite using a Box-Behnken experimental design. Open Chem. 16, 992–1000. https://doi.org/10.1515/chem-2018-0114.

Varank, G., Demir, A., Top, S., Sekman, E., Bilgili, M., 2012. Removal of 4-nitrophenol from aqueous solution by natural low-cost adsorbents, Indian. J. Chem. Technol. 19, 7–25.

Wang, W., Zhang, L., Li, Z., Zhang, S., Wang, C., Wang, Z., 2016. A nanoporous carbon material derived from pomelo peels as a fiber coating for solid-phase microextraction. RSC Adv. 6, 113951–113958. https://doi.org/10.1039/c6ra24225a.

Wu, C., Zhao, B., Li, Y., Wu, Q., Wang, C., Wang, Z., 2011a. Development of dispersive liquid-liquid microextraction based on solidification of floating organic drop for the sensitive determination of trace copper in water and beverage samples by flame atomic absorption spectrometry. Bull. Korean Chem. Soc. 32, 829–835. https://doi.org/10.5012/bkcs.2011.32.3.829.

Wu, Q., Wu, C., Wang, C., Lu, X., Li, X., Wang, Z., 2011b. Sensitive determination of cadmium in water, beverage and cereal samples by a novel liquid-phase microextraction coupled with flame atomic absorption spectrometry. Anal. Methods. 3, 210–216. https://doi.org/10.1039/C0AY00524J.

Yadav, S.K., Singh, D.K., Sinha, S., 2014. Chemical carbonization of papaya seed originated charcoals for sorption of Pb (II) from aqueous solution. J. Environ. Chem. Eng. 2, 9–19. https://doi.org/10.1016/j.jece.2013.10.019.

Yargıç, A.Ş., Yarbay Şahin, R.Z., Özbay, N., Önal, E., 2015. Assessment of toxic copper(II) biosorption from aqueous solution by chemically-treated tomato waste. J. Clean. Prod. 88, 152–159. https://doi.org/10.1016/j.jclepro.2014.05.087.

Yu, C., Shao, J.C., Sun, W.J., Yu, X.N., 2020. Treatment of lead contaminated water using synthesized nano-iron supported with bentonite/graphene oxide. Arab. J. Chem. 13, 3474–3483. https://doi.org/10.1016/j.arabjc.2018.11.019.

Zvinowanda, C.M., Okonkwo, J.O., Agyei, N.M., Staden, M.V., Jordaan, W., Kharebe, B.V., 2010. Recovery of Lead (II) from Aqueous Solutions by Zea mays Tassel Biosorption. Am. J. Biochem. Biotechnol. 6 (1), 1–10. https://doi.org/10.3844/ajbbsp.2010.1.10.